Supporting Information for

Electronic Regulation of Carbon Site by Oxygenated Groups for Electrochemical Oxygen Reduction to H_2O_2

Yin Wang[1*, a], Tingting Zhang[1, a], Dongyong Li[1, a], Peihe Li[a], Quanli Hu[a], Quan Zhuang*[, a], Limei Duan[a], Jinghai Liu*[, a]

[a]Inner Mongolia Key Laboratory of Solid State Chemistry for Battery, Inner Mongolia Engineering Research Center of Lithium-Sulfur Battery Energy Storage, College of Chemistry and Materials Science, Inner Mongolia Minzu University, Tongliao 028000, People's Republic of China.

[1]These authors contributed equally to this work

E-mail: *ywang@imun.edu.cn*; *jhliu2015@imun.edu.cn*; *zhuangquan21@outlook.com*

Experimental sections

Materials

All the chemical reagents were used directly without further purification. Ketjen Black (KB, Carbon ECP 600JD) was purchased from Lion Corporation. Supper P (SP) was purchased from TIMCAL Graphite & Carbon. Graphite Carbon (GC) was purchased from Wuxi Hengtai Metal Materials Co., Ltd.. Nafion aqueous (5 wt% in water) was purchased from Dupont Corporation. Potassium hydroxide (KOH), sulphuric acid (H_2SO_4, 98%), hydrogen peroxide aqueous (H_2O_2, 30 wt% in water), cerium sulfate ($Ce(SO_4)_2$) were purchased from Sinopharm Chemical Reagent Co. Ltd..

Synthesis of KB-Ox

1 g of KB was mixed with 2 mL of deionized water, then the mixture was placed into a tube furnace and heated to 350 ^oC under air atmosphere for 2 h, the heating rate was 5 ^oC/min. After cooling down to the room temperature naturally, the KB-Ox was obtained.

Synthesis of KB-Re

1 g of KB was placed into a tube furnace and heated to 1100 ^oC under Ar atmosphere for 2 h, the heating rate was 5 ^oC/min. After cooling down to the room temperature naturally, the KB-Re was obtained.

Synthesis of KB-Ox2, KB-Re2, SP-Ox and GC-Ox

KB-Ox2 was synthesized as the method of KB-Ox with the KB-Re as the precursor. KB-Re2 was synthesized as the method of KB-Re with the

KB-Ox as the precursor.

SP-Ox and GC-Ox were synthesized as the preparation of KB-Ox using SP and GC as the precursors.

Physical and chemical characterizations

Scanning electron microscope (SEM) was performed on a S4800 (HITACHI) at an accelerating voltage of 5 kV. Transmission electron microscope (TEM) was measured on a JEM-F200 (JEOL) at an accelerating voltage of 200 kV. N_2 adsorption-desorption isotherms were recorded on a Quadrasorb SI (Quantachrome). The specific surface area was analyzed by the method of Brunauer-Emmett-Teller (BET), the pore distribution was calculated by the non-local density functional theory (NLDFT) method. X-ray diffraction (XRD) pattern was recorded on a SmartLab (Rigaku) with graphite-monochromatized Cu Ka radiation (9 kW, λ = 0.1541 nm; scan speed of 6 °/min; 2θ = 10-80 °) at room temperature. Raman spectra were recorded on an Invia (Renishaw) with a 632 nm laser (scanning range of 1000-2000 cm^{-1}). NH_3 temperature programmed desorption (NH_3-TPD) were carried out on a ChemBET (Quantachrome) with the desorption temperature of 50-800 ^oC. Oxygen (O_2) adsorption isotherms were recorded on an aperture analyzer (ASAP2460, Micromeritics) at 25 °C. X-ray photoelectron spectroscopy (XPS) measurements were conducted on an AXIS SUPRA (Kratos) using Al Kα radiation as the X-ray source (1486.7 eV) with the pass energy of

30 eV. Static water contact angles were recorded on a JC8000DM (Shanghai Zhongchen Digtal Technology Apparatus Co., Ltd.). Element analysis (EA) were carried out using a Vario EL cube elemental analyzer. Electron paramagnetic resonance (EPR) were conducted on an EMX Plus (Bruker) under ambient room temperature.

Electrode preparations

Electrochemical 2eORR measurements were performed through a rotating ring disk electrode (RRDE, AFE6R2GCPT, disk area: 0.2375 cm^2, ring area: 0.2356 cm^2, collection efficiency: 38 %). H_2O_2 productions were carried out in a H-type cell with a carbon paper (CP, NOS1005, CeTech) as the working electrode.

RRDE preparation: 2 mg of catalyst was dispersed into a mixed solution (700 μL deionized water, 270 μL ethanol and 30 μL Nafion aqueous), and a homogeneous suspension ink was obtained after the mixture sonicated for 4 h. Then, 10 μL of suspension ink was dropped onto the risk electrode and dried under ambient condition. The loading mass of catalyst on the risk electrode is 0.08 mg cm^{-2}.

CP preparation: 8 mg of KB-Ox was dispersed into a mixed solution (950 μL ethanol and 50 μL Nafion) by sonication for 1 h to form a homogeneous ink. Then, 50 μL of the catalyst ink was dropped onto a 1 × 1 cm of CP and dried under ambient condition. The loading mass of catalyst on the CP is 0.4 mg cm^{-2}.

Electrochemical characterization

Electrochemical tests were performed on a Bio-Logic VMP-3 multichannel electrochemical workstation. The RRDE with catalyst was used as the working electrode, a Pt wire as the counter electrode and a KCl saturated Ag/AgCl as the reference electrode. A 0.1 mol/L KOH solution (pH = 13) was used as the ORR electrolyte. Firstly, 10 cycles of cyclic voltammetry (CV) in N_2-saturated electrolytes were performed on disk electrode with the sweeping potential between 0.2 V and 1.3 V vs. reversible hydrogen electrode (RHE). The scan rate was 100 mV s^{-1}. Then, the electrolyte was purged with O_2 for 30 min before ORR test, the oxygen reduction current of disk electrode was measured by linear sweep voltammetry (LSV) with the potential from 1.3 V to 0.2 V vs. RHE at a scan rate of 5 mV s^{-1}. During the testing process, a constant potential of 1.2 V vs. RHE was applied on the ring electrode to test the H_2O_2 formed on the disk electrode, the H_2O_2 oxidation current of ring electrode was used to evaluate the ORR selectivity. The rotation speed of RRDE is setup to 1600 rpm. The transferred electrons transfer number (n_{RRDE}) and the H_2O_2 yield of catalysts were calculated as the follow equations:

$$n_{RRDE} = 4\frac{I_D}{I_D + I_R/N} \quad (1)$$

$$H_2O_2\ yield\ (\%) = 200\frac{I_R/N}{I_D + I_R/N} \quad (2)$$

I_R is the ring current, I_D is the disk current and N is the collection

efficiency (N = 0.38) of RRDE.

The potential vs. RHE is calculated according to the Nernst equation as follow:

$$E(vs.RHE) = E(vs.Ag/AgCl) + 0.197 + 0.0592 * pH \quad (3)$$

H_2O_2 concentration measurements

Electrocatalytic H_2O_2 production was performed in an H-type cell with a Nafion 211 membrane as the separator between the cathode cell and anode cell. Each cell was filled with 35 mL 0.1 M KOH as the electrolyte. For the cathode compartment, the as-prepared carbon paper as the working electrode and a KCl saturated Ag/AgCl electrode as the reference electrode. For the anode compartment, a Pt sheet (1 × 1 cm) electrode as the counter electrode. Before the electrochemical test, O_2 was bubbled into the cathode compartment for 30 min removing the air. The chronoamperometry method was used to produce H_2O_2, a potential of 0.5 V versus RHE was applied.

The H_2O_2 concentration was measured by an ultraviolet-visible (UV-Vis) spectrometry (UV2310II, Techcomp) with a cerium sulfate ($Ce(SO_4)_2$) solution (100 mM of $Ce(SO_4)_2$) as the chromogenic reagent. 1 mL of catholyte after electrochemical test and 3 mL of $Ce(SO_4)_2$ solution were mixed and placed under dark condition for 10 min, the mixed solution was measured using the UV-Vis spectrometry between 420 ~ 540 nm, the absorbance at 480 nm was used to calculate the H_2O_2 concentration

according to the calibration curve (Figure S4). The H_2O_2 faradaic efficiency (FE_{H2O2}) was calculated as the equation 4:

$$FE_{H2O2} = \frac{2 \times F \times C_{H2O2} \times V}{Q} \times 100\% \quad (4)$$

Where C_{H2O2} is the measured molar concentration of H_2O_2 (mmol/L), V is the volume of electrolyte in cathode chamber (0.035 L), F is the Faraday constant (96485 C/mol) and Q is the total charge passed during the electrocatalytic reaction.

Computational Methods

The density functional theory (DFT) calculations were performed using Vienna *ab initio* Simulation Package (VASP).[1] The interaction between electron and ion nuclei is described by using the projected augmented wave (PAW) method.[2] The Bayes error estimation function and van der Waals correlation (BEEF-vdW) function are adopted to precisely describe the properties on graphene.[3] The plane-wave kinetic energy cutoff of 400 eV with a Gaussian smearing width of 0.1 eV, and Monkhorst–Pack *k*-point grids of 1 × 4 × 1 were adopted to ensure the convergence of the total-energy calculations. Furthermore, the convergence for total energy and interaction force was set to be 10^{-4} eV and 10^{-2} eV $Å^{-1}$, respectively. The structure of the model was constructed by connecting different functional groups (-OH, -CHO, -COOH) on the edge of 4 × 5 supercell of a single layer graphite orthogonal single cell, along with a vacuum layer of 20 Å in the Z direction to avoid periodic interactions. Device Studio program provides a number of functions for performing visualization, modeling and simulation.[4] The electronic localized function (ELF) and electronic density states (DOS) were performed by DS-PAW software integrated in Device

Studio program.[5]

The model structures were used to model the 2eORR reaction pathway:

$$OOH^* + (H^+ + e^-) \rightarrow H_2O_2 + * \quad (1)$$

$$O_2 + * + (H^+ + e^-) \rightarrow OOH^* \quad (2)$$

Where * represents the active sites. The overpotential is determined by either the first proton-electron transfer to form OOH* or the second electron transfer to form H_2O_2. Obviously, the intermediate OOH* plays a key role in the 2eORR.

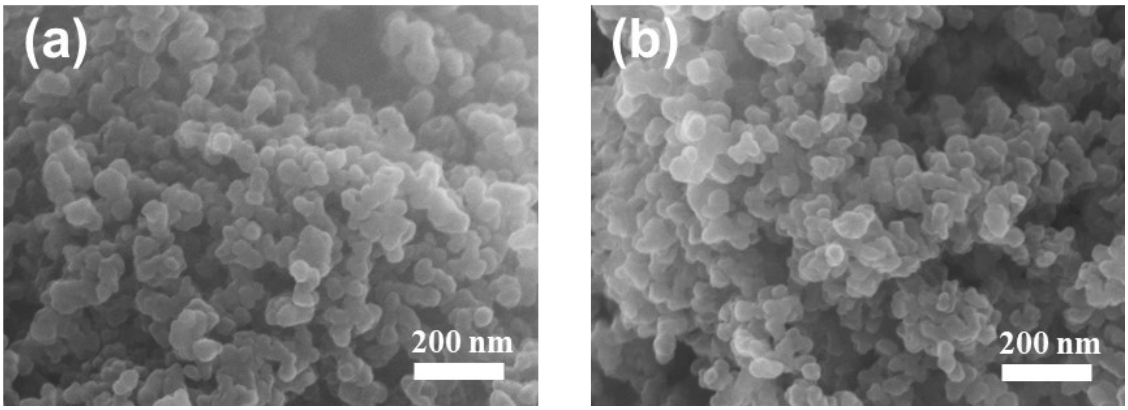

Figure S1. SEM images of (a) KB and (b) KB-Re

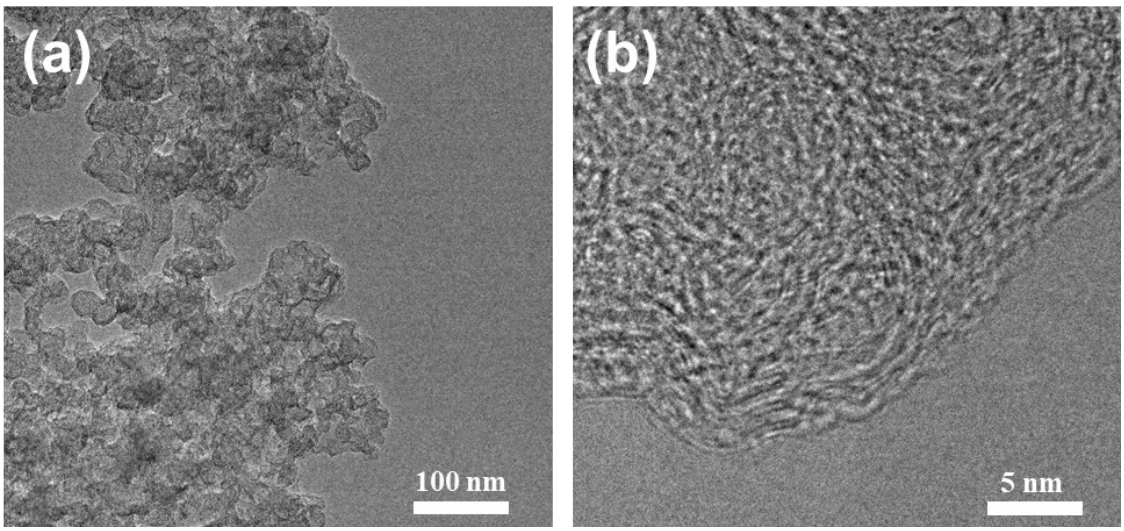

Figure S2. (a) TEM image and (b) HRTEM image of KB.

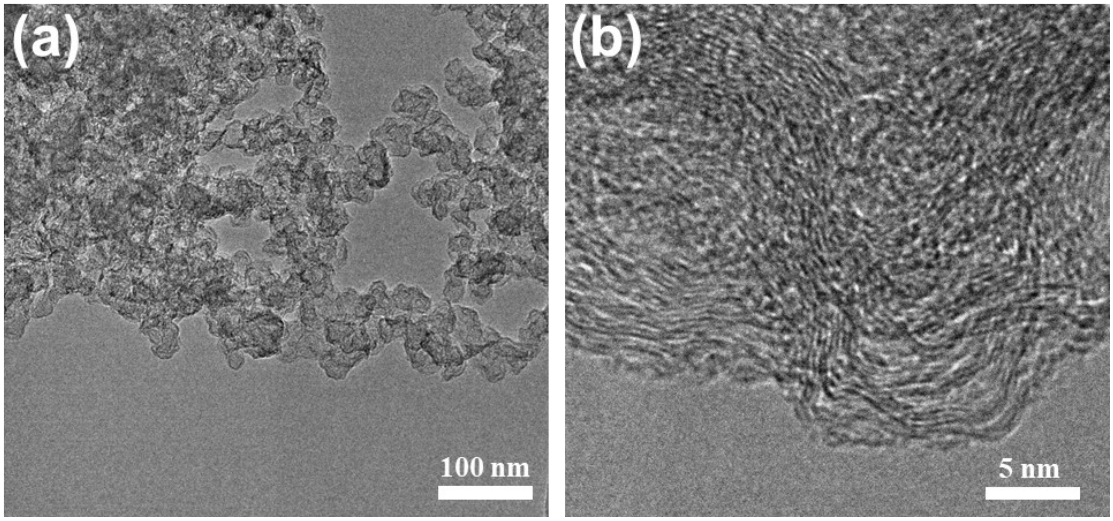

Figure S3. (a) TEM image and (b) HRTEM image of KB-Re.

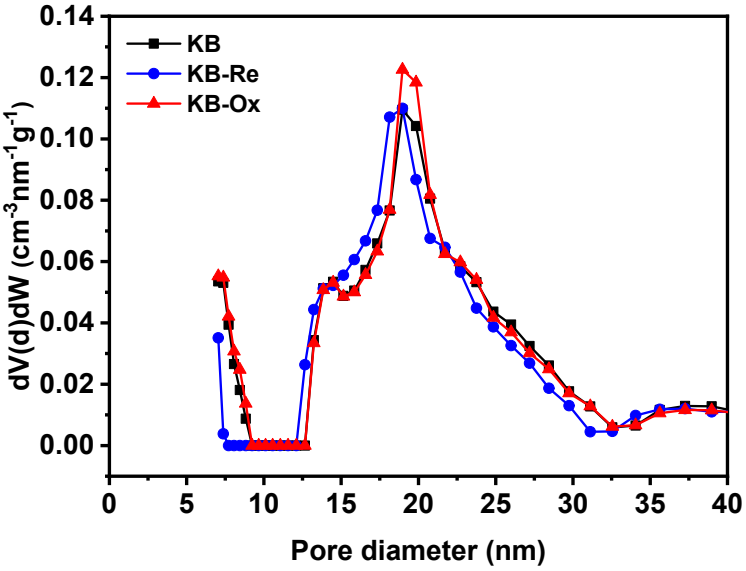

Figure S4. Pore size distributions of KB, KB-Re and KB-Ox.

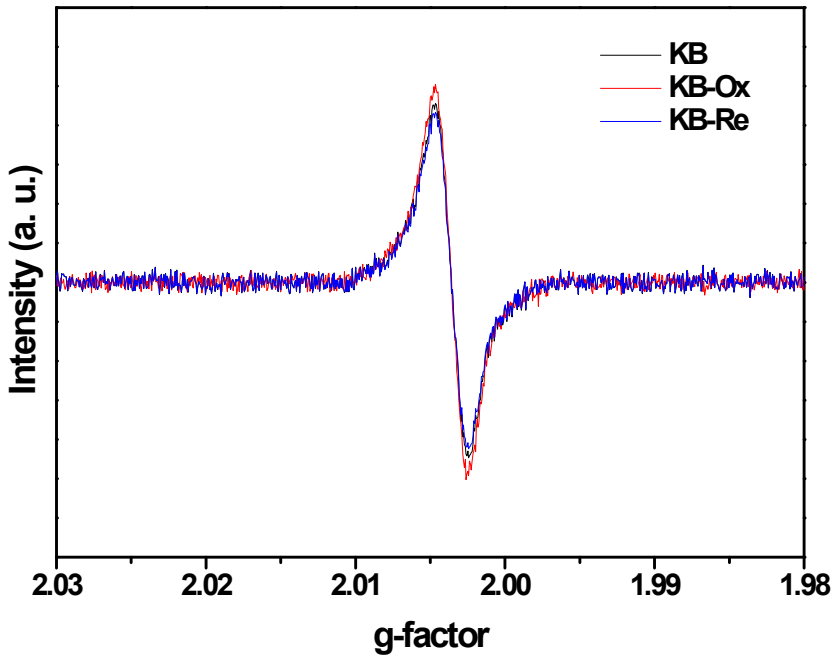

Figure S5. EPR spectra of KB, KB-Re and KB-Ox.

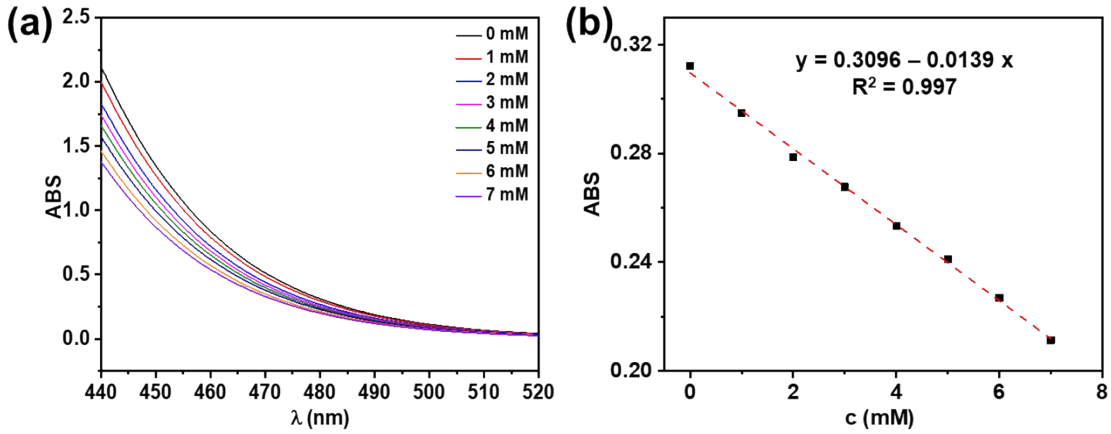

Figure S6. (a) UV-Vis spectra and (b) the calibration curve for standard solutions of H_2O_2.

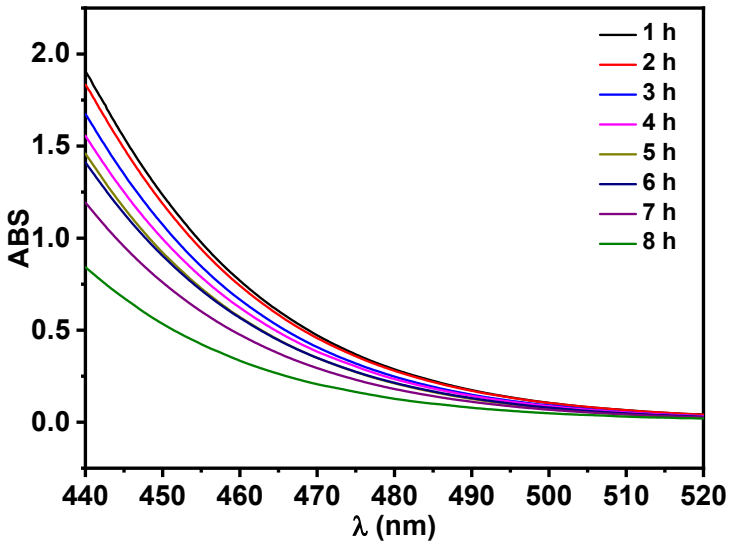

Figure S7. UV-Vis spectra of H_2O_2 during 8 h electrolysis.

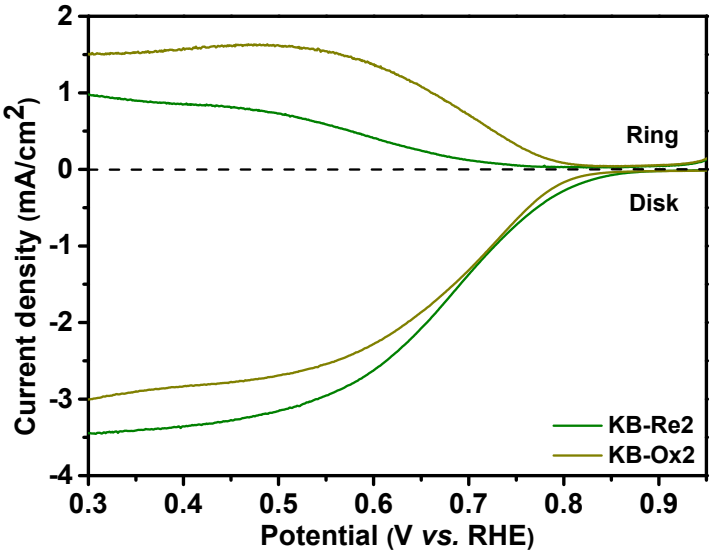

Figure S8. RRDE voltammograms at 1600 rpm in O_2-saturated 0.1 mol/L KOH electrolyte of KB-Re2 and KB-Ox2.

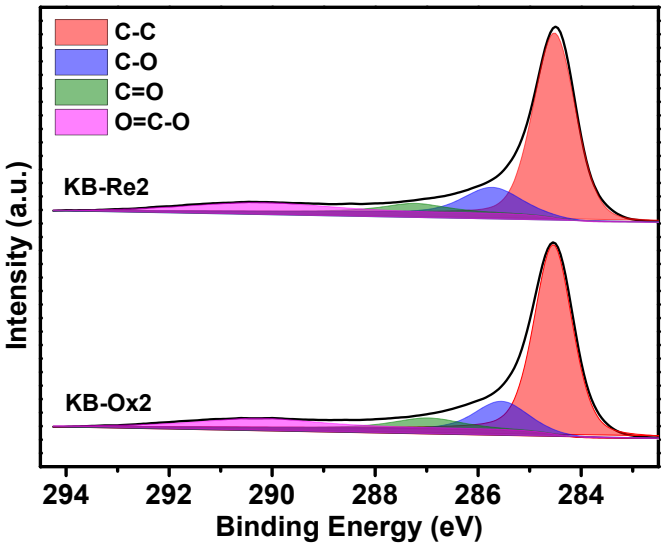

Figure S9. C 1s XPS spectra of KB-Re2 and KB-Ox2.

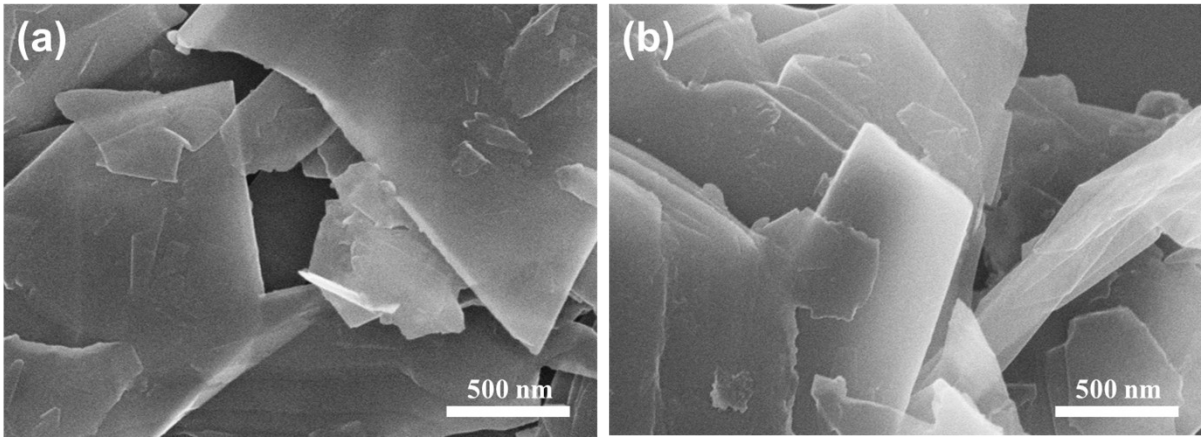

Figure S10. SEM images of (a) GC and (b) GC-Ox.

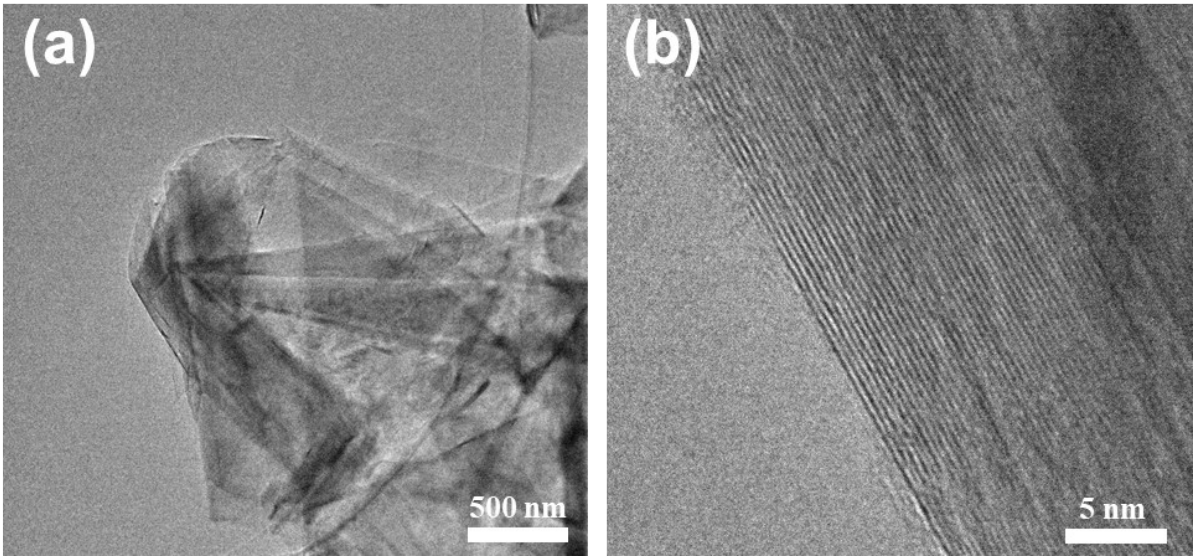

Figure S11. (a) TEM image and (b) HRTEM image of GC.

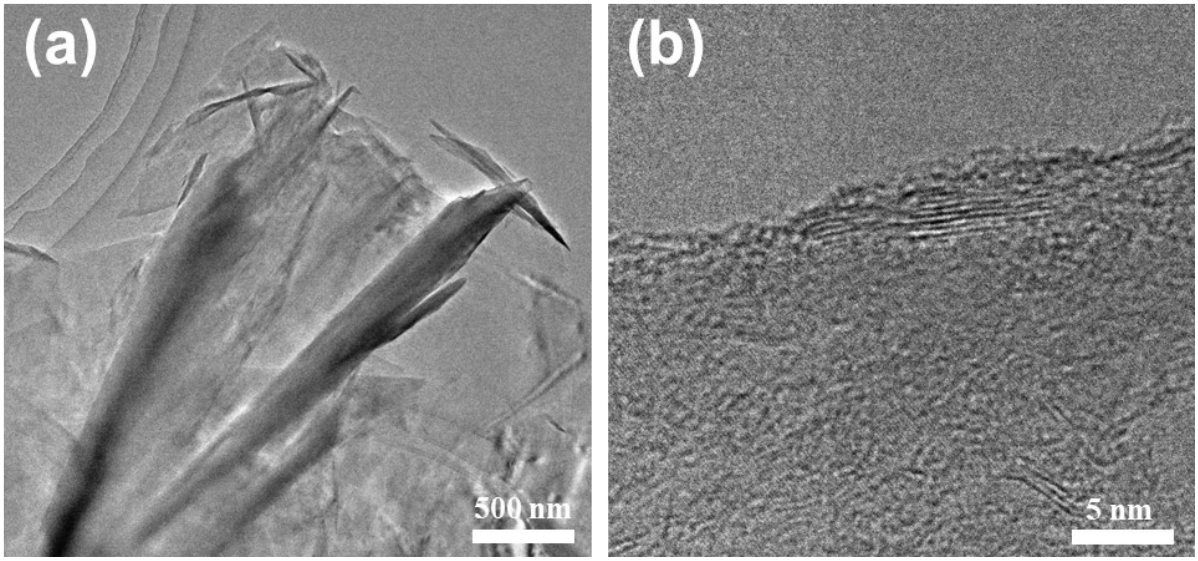

Figure S12. (a) TEM image and (b) HRTEM image of GC-Ox.

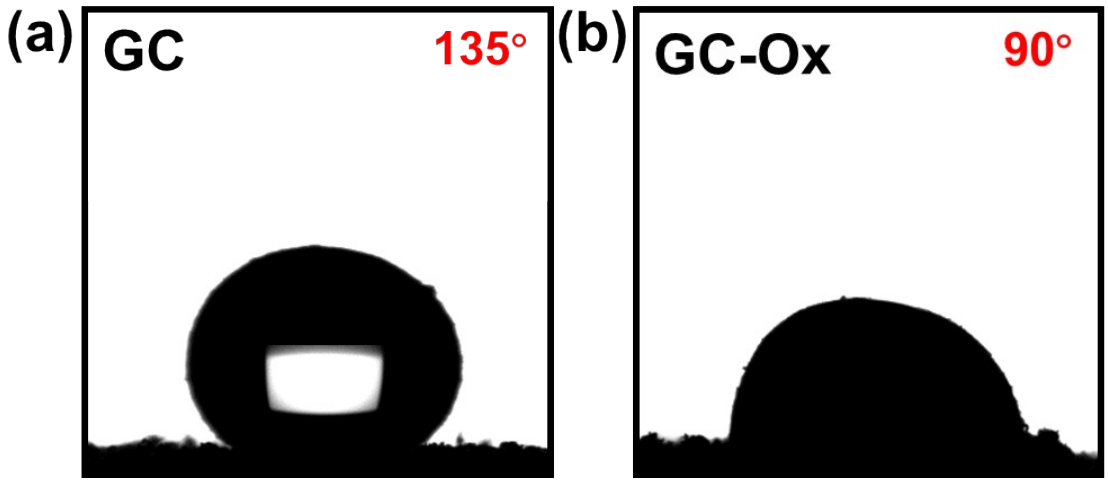

Figure S13. Contact angles with 0.1 mol/L KOH solution of (a) GC and (b) GC-Ox.

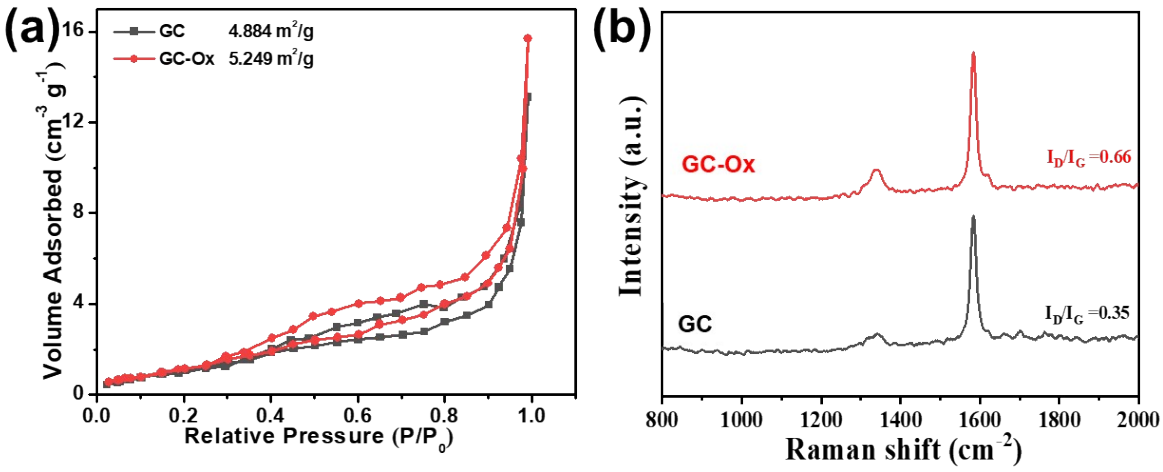

Figure S14. (a) N_2 adsorption-desorption isothermals and (b) Raman spectra of GC and GC-Ox.

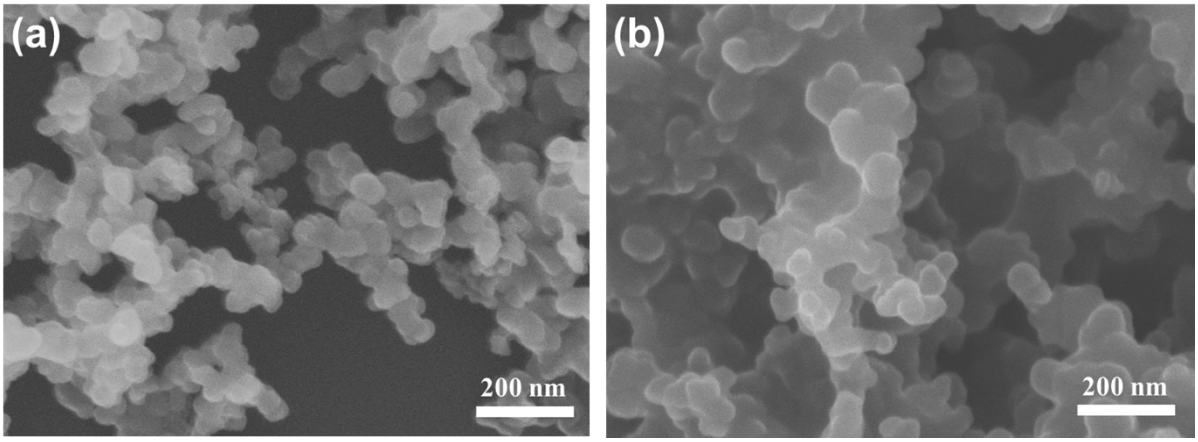

Figure S15. SEM images of (a) SP and (b) SP-Ox.

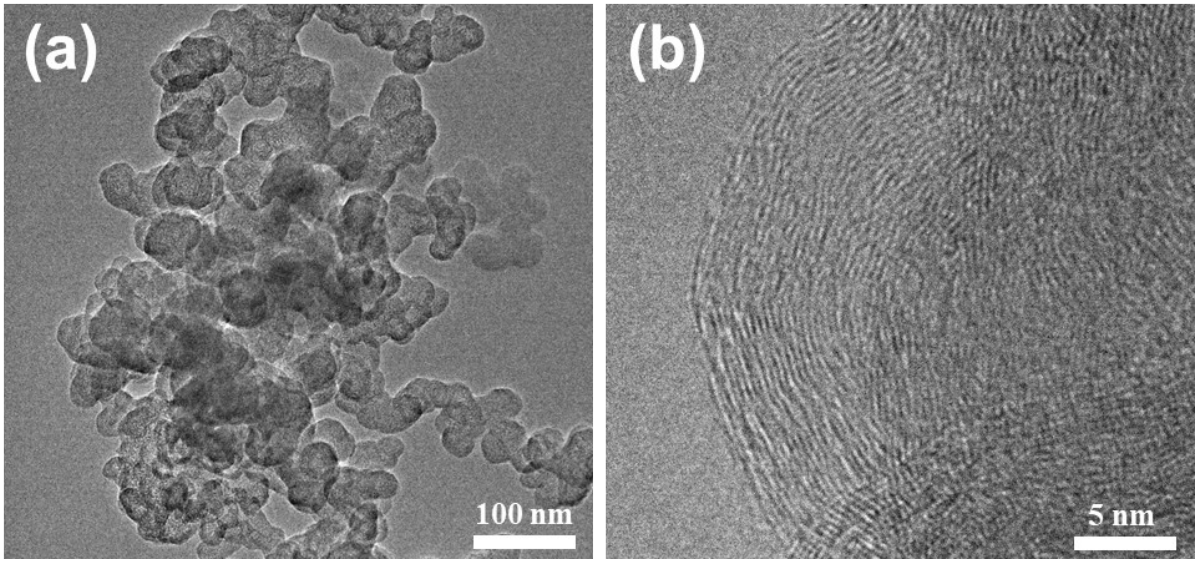

Figure S16. (a) TEM image and (b) HRTEM image of SP.

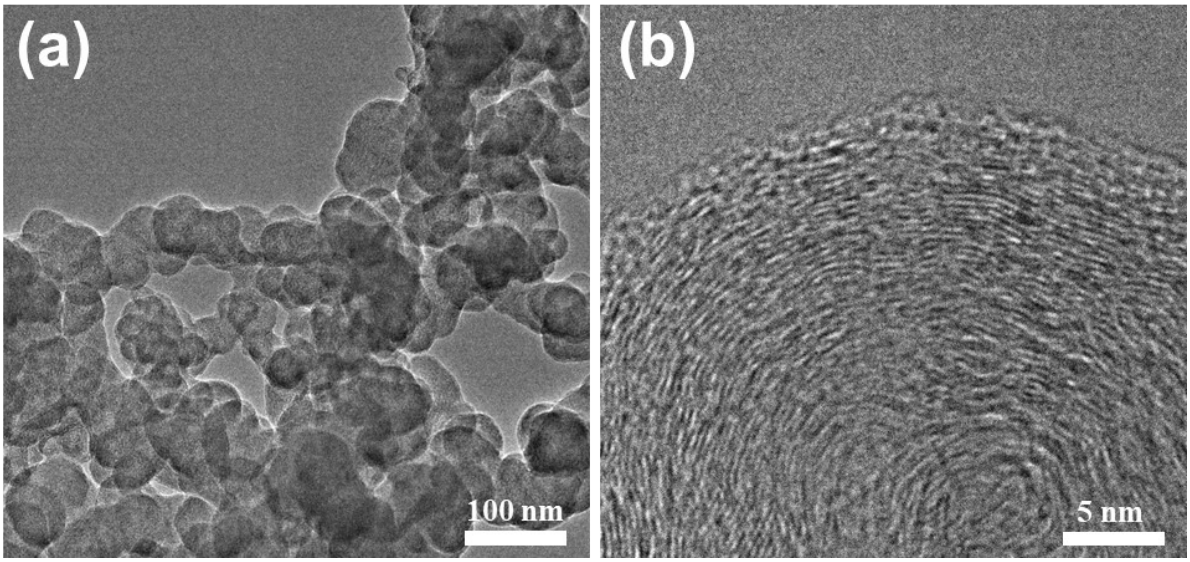

Figure S17. (a) TEM image and (b) HRTEM image of SP-Ox.

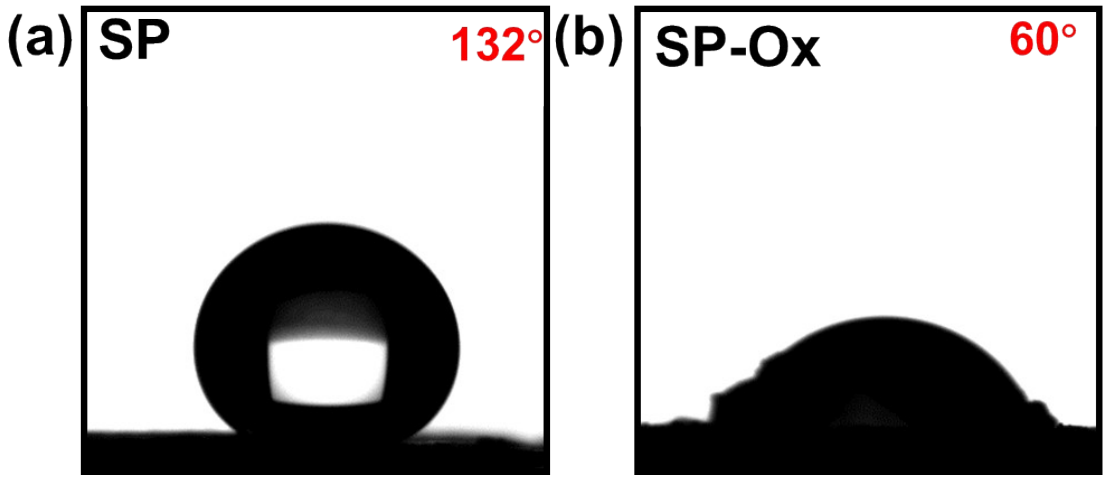

Figure S18. Contact angles with 0.1 mol/L KOH solution of (a) SP and (b) SP-Ox.

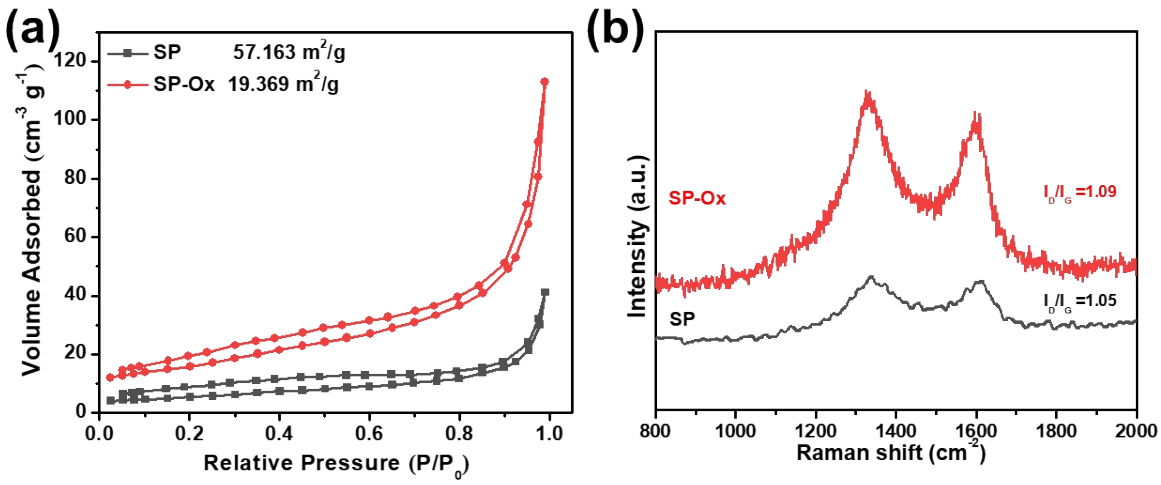

Figure S19. (a) N_2 adsorption-desorption isothermals and (b) Raman spectra of SP and SP-Ox.

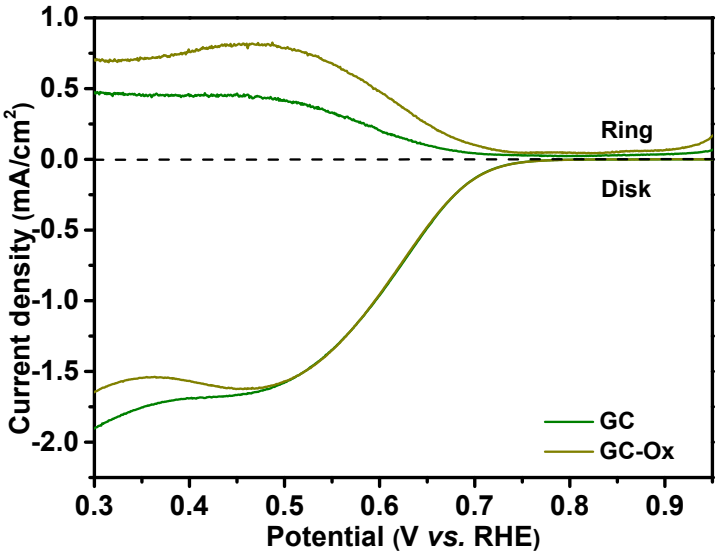

Figure S20. RRDE voltammograms at 1600 rpm in O_2-saturated 0.1 mol/L KOH electrolyte of GC and GC-Ox.

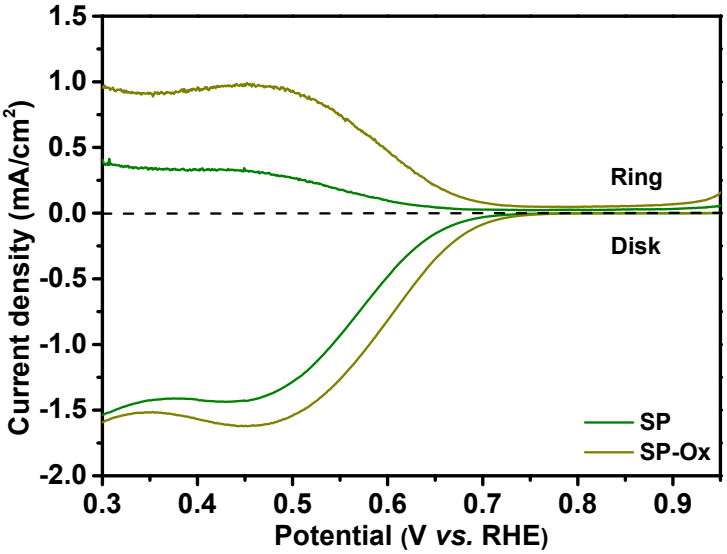

Figure S21. RRDE voltammograms at 1600 rpm in O_2-saturated 0.1 mol/L KOH electrolyte of SP and SP-Ox.

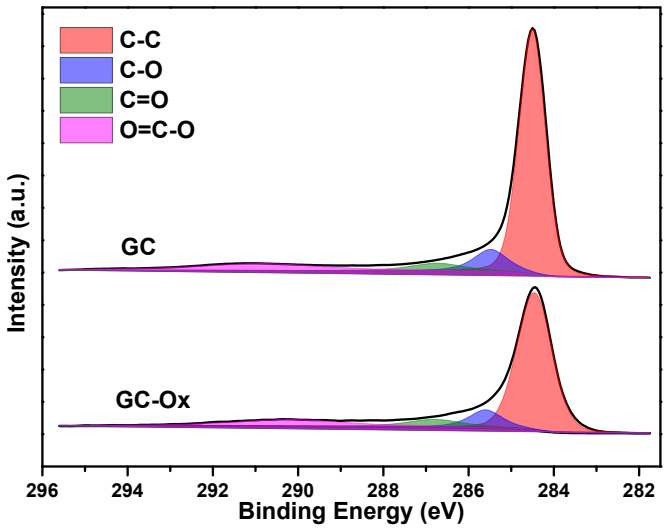

Figure S22. C 1s XPS spectra of GC and GC-Ox.

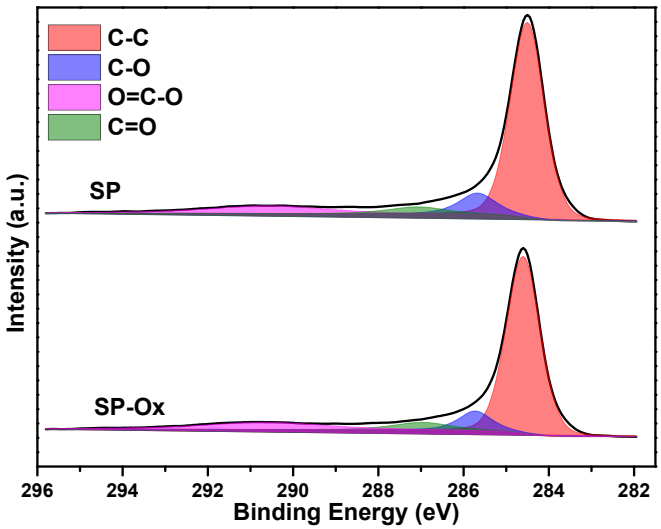

Figure S23. C 1s XPS spectra of SP and SP-Ox.

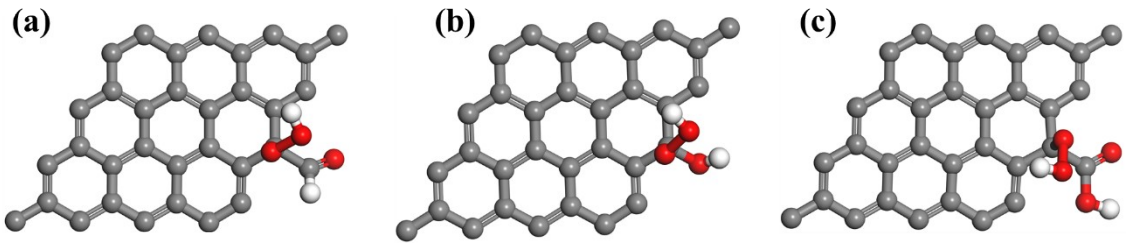

Figure S24. The OOH* adsorption model onto the configurations of (a) Edge-CHO, (b) Edge-OH and (c) Edge-COOH. Color code: C, gray; O, red; H, white.

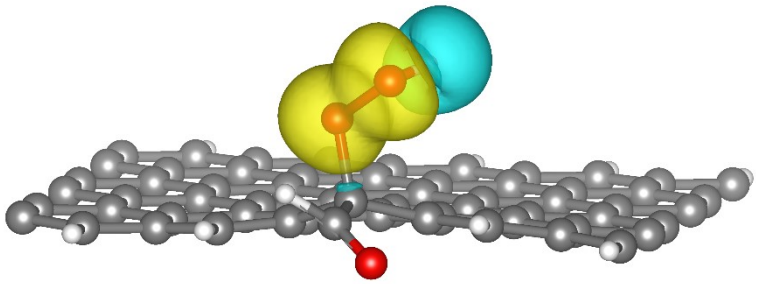

Figure S25. Differential charge densities of the Edge-CHO model with highest 2eORR activity. Cyan and yellow isosurfaces donating electron losing and gaining, respectively.

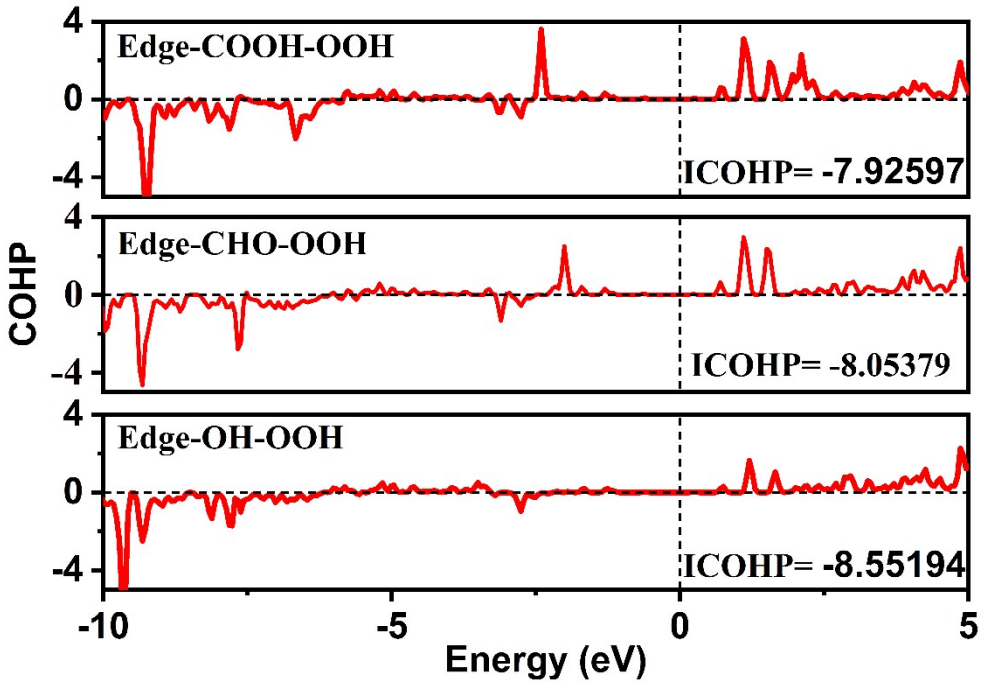

Figure S26. The COHP for C-O interactions for -OOH adsorption on Edge-CHO, Edge-OH and Edge-COOH. Bonding and antibonding states are shown on the bottom and top, respectively.

Table S1. Element compositions determined by element analysis (EA) and X-ray photoelectron spectroscopy (XPS) of KB, KB-Ox and KB-Re

Method	EA			XPS		
Element	C (at%)	O (at%)	O/C (at/at)%	C (at%)	O (at%)	O/C (at/at)%
KB	97.5	2.5	2.56	98.6	1.4	1.42
KB-Ox	96.1	3.9	4.03	97.8	2.1	2.15
KB-Re	98.2	1.8	1.84	98.9	1.1	1.11

Reference

1 G. Kresse and J. Furthmuller, *Phys. Rev. B*, 1996, **54**, 11169-11186.

2 G. Kresse and D. Joubert, *Phys. Rev. B*, 1999, **59**, 1758-1775.

3 J. Wellendorff, K. T. Lundgaard, A. Møgelhøj, V. Petzold, D. D. Landis, J. K. Nørskov, T. Bligaard and K. W. Jacobsen, *Phys. Rev. B*, 2012, **85**, 235149.

4 Device Studio, Version 2023A, Hongzhiwei Technology, China, 2024, Available online: https://iresearch.net.cn/cloudSoftware accessed on March, 10.

5 P. E. Blöchl, *Phys. Rev. B*, 1994, **50**, 17953-17979.